Supporting Information

Effect of Molecule-Substrate Interaction on the Adsorption of *meso*-Dibenzoporphycene Tautomers Studied by Scanning Probe Microscopy and First-Principles Calculations

Tomoko K. Shimizu,[1,2] *Carlos Romero-Muñiz,*[3,4] *Oleksandr Stetsovych,*[2,5] *Jaime Carracedo-Cosme,*[3,6] *Michael Ellner,*[3] *Pablo Pou,*[3,7] *Koji Oohora,*[8] *Takashi Hayashi,*[8] *Ruben Perez,*[3,7*] *Oscar Custance*[2*]

1. Department of Applied Physics and Physico-Informatics, Faculty of Science and Technology, Keio University, 3-14-1 Hiyoshi, Kohoku, Yokohama, Kanagawa 223-8522, Japan.

2. National Institute for Materials Science, 1-2-1 Sengen, Tsukuba, Ibaraki, 305-0047, Japan.

3. Departamento de Física Teórica de la Materia Condensada, Universidad Autónoma de Madrid, E-28049 Madrid, Spain.

4. Department of Physical, Chemical and Natural Systems, Universidad Pablo de Olavide, Ctra. Utrera Km. 1, E-41013, Seville, Spain.

5. Institute of Physics, Academy of Sciences of the Czech Republic, Cukrovarnická 10, 162 00 Prague 6, Czech Republic.

6. Quasar Science Resources S.L., Camino de las Ceudas 2, E-28232 Las Rozas de Madrid, Spain.

7. Condensed Matter Physics Center (IFIMAC), Universidad Autónoma de Madrid, E-28049 Madrid, Spain.

8. Department of Applied Chemistry, Graduate School of Engineering, Osaka University, 2-1 Yamadaoka, Suita, Osaka, 565-0871 Japan.

Theoretical details

We have performed density functional theory calculations using the plane-wave code VASP.[1] An energy cutoff for the basis set of 400 eV was used in combination with pseudopotentials constructed with the PAW method.[2,3] The Perdew-Burke-Ernzerhof functional[4] was employed to reproduce the electronic exchange and correlation, supplemented by the D3 semi-empirical correction[5] to account for the dispersion interactions. We have studied the adsorption of the mDBPc molecule on Ag(111) and NaCl(100). In order to simulate the substrate, we use simple rigid slabs consisting of 9×7 (three layers) and 6×6 (two layers) supercells respectively. The most favorable adsorption sites were found for each conformer after exploring the energetic landscape through the $x - y$ plane. Due to the high symmetry of the substrates, this is a suitable approach, which provides a preliminary picture of the energy landscape. In the case of NaCl, we considered two different orientations, one aligned with the [100] direction and the other rotated by 45º, that led us to the basic identification of the adsorption configurations B and A, respectively. Subsequently, all the structures were fully relaxed, keeping the substrate atoms fixed, following a conjugate gradient algorithm until forces upon atoms were smaller than 0.01 eV/Å, while each electronic self-consistent loop was calculated with a precision of 10^{-5} eV. A vertical vacuum region larger than 10 Å was established between periodical images, and a dipole correction along the *z*-axis was also used. The adsorption energy of the mDPBc molecule was calculated in both substrates as: E_{ad} = E[mol+slab] – E[mol] – E[slab], where E[mol+slab] is the energy of the whole system and E[mol] and E[slab] are the energies of the relaxed and isolated molecule and slab respectively. The Climbing Image Nudged Elastic Band (CI-NEB) method[6] has been used to find the minimum-energy paths for the on-surface tautomerization processes. In these calculations the convergence criterion in forces was 0.05 eV Å, and a spring constant of 1.5 eVÅ^{-2} was employed

between the intermediate images considered during the calculations. According to previous references by Kumagai and coworkers,[7,8] the zero-point energy (ZPE) correction to the transition state energy could affect the final result remarkably. This correction is made using the energy of the vibrational modes associated to the amine groups. As described in those references, we have performed the dynamic calculations necessary to account for this effect, and we have confirmed that the influence of ZPE is negligible in our case and it does not affect our final conclusions. In particular, we have found that the barrier in configuration A is lowered by 7 meV considering the ZPE correction, and that the barriers involved in the configuration B remain unchanged (with a ZPE less than 0.5 meV).

From the DFT calculations described above, we use our recently developed method to simulate the AFM images.[9] A detailed description of this method can be found in our previous works.[9,10,11] In brief, the method is based on a total potential $V(R_{tip})$, obtained from four separated contributions: electrostatic V_{ES}, short range V_{SR}, van der Waals V_{vdW} and tilting V_{tilt}.The first two contributions are obtained from the total charge densities of probe and sample ($\rho^{tip}$and ρ^{sam}), and the electrostatic potential of the sample ϕ^{sam}, which are obtained from a previous plane-wave calculation of the system without the probe. These contributions are calculated using the following expressions:

$$V_{ES} = \int \rho^{tip}(\boldsymbol{r}, R_{tip})\phi^{sam}(\boldsymbol{r})d\boldsymbol{r},$$

$$V_{SR} = V_0 \int \left[\rho^{tip}(\boldsymbol{r}, R_{tip})\rho^{sam}(\boldsymbol{r})\right]^{\alpha} d\boldsymbol{r},$$

where α and V_0 are two fitting parameters specific to the system. In our particular case $\alpha = 1.07$ and V_0=13.36 [eV].* On the other hand, the van der Waals contribution is extracted from the D3 estimation provided in the DFT calculation, while the tilt potential is given by

$$V_{tilt} = \frac{1}{2}k'(\Delta x^2 + \Delta y^2),$$

where $k'$is a spring constant chosen to improve the matching with the experimental images. In our case, we have set $k' = 0.46\ \mathrm{Jm}^{-2}$. This last term accounts for the possible probe's orientations. Notice that, instead of performing a direct minimization of the CO tilting taking into account the orientation change of the whole CO charge density as done in previous works,[9,10,11] we have proceeded with a more efficient approximation valid for small angles. Similar to P. Hapala, *et al.*,[12,13] we minimize the total energy for small displacements in xy around the initial position of the apex, considering a rigid probe and restricting the movement to the original plane. This approach speeds up the simulations an order of magnitude with small accuracy loss. We have chosen the simulated force maps to make the comparison with the experimental AFM images instead of the gradient force images. This is because the typical experimental amplitudes produce non-negligible variations on the gradient with respect to the probe-sample distance during the oscillation cycles.

References

(1) Kresse, G.; Furthmüller, J. Efficient Iterative Schemes for Ab Initio Total-Energy Calculations Using a Plane-Wave Basis Set. *Phys. Rev. B* **1996**, *54*, 11169–11186.

(2) Blöchl, P. E. Projector Augmented-Wave Method. *Phys. Rev. B* **1994**, *50*, 17953–17979.

(3) Kresse, G.; Joubert, D. From Ultrasoft Pseudopotentials to the Projector Augmented-Wave Method. *Phys. Rev. B* **1999**, *59*, 1758–1775.

* Notice that V_0 depends nontrivially on the units of the charge density; here, all charge densities are given in e/Å^3 and energies in eV, so we use [eV] to depict this choice.

(4) Perdew, J. P.; Burke, K.; Ernzerhof, M. Generalized Gradient Approximation Made Simple. *Phys. Rev. Lett.* **1996**, *77*, 3865–3868.

(5) Grimme, S.; Antony, J.; Ehrlich, S.; Krieg, H. A Consistent and Accurate Ab Initio Parametrization of Density Functional Dispersion Correction (DFT-D) for the 94 Elements H-Pu. *J. Chem. Phys.* **2010**, *132*, 154104.

(6) Henkelman, G.; Uberuaga, B. P.; Jónsson, H. Climbing Image Nudged Elastic Band Method for Finding Saddle Points and Minimum Energy Paths. *J. Chem. Phys.* **2000**, *113*, 9901–9904.

(7) Ladenthin, J. N.; Frederiksen, T.; Persson, M.; Sharp, J. C.; Gawinkowski, S.; Waluk, J.; Kumagai, T. Force-Induced Tautomerization in a Single Molecule. *Nat. Chem.* **2016**, *8*, 935–940.

(8) Koch, M.; Pagan, M.; Persson, M.; Gawinkowski, S.; Waluk, J.; Kumagai, T. Direct Observation of Double Hydrogen Transfer via Quantum Tunneling in a Single Porphycene Molecule on a Ag(110) Surface. *J. Am. Chem. Soc.* **2017**, *139*, 12681–12687.

(9) Ellner, M.; Pou, P.; Pérez, R. Molecular Identification, Bond Order Discrimination, and Apparent Intermolecular Features in Atomic Force Microscopy Studied with a Charge Density Based Method. *ACS Nano* **2019**, *13*, 786–795.

(10) Ellner, M.; Pavliček, N.; Pou, P.; Schuler, B.; Moll, N.; Meyer, G.; Gross, L.; Peréz, R. The Electric Field of CO Tips and Its Relevance for Atomic Force Microscopy. *Nano Lett.* **2016**, *16*, 1974–1980.

(11) Ellner, M.; Pou, P.; Pérez, R. Atomic Force Microscopy Contrast with CO Functionalized Tips in Hydrogen-Bonded Molecular Layers: Does the Real Tip Charge Distribution Play a Role? *Phys. Rev. B* **2017**, *96*, 075418.

(12) Hapala, P.; Kichin, G.; Wagner, C.; Tautz, F. S.; Temirov, R.; Jelínek, P. Mechanism of High-Resolution STM/AFM Imaging with Functionalized Tips. *Phys. Rev. B* **2014**, *90*, 085421.

(13) Hapala, P.; Temirov, R.; Tautz, F. S.; Jelínek, P. Origin of High-Resolution IETS-STM Images of Organic Molecules with Functionalized Tips. *Phys. Rev. Lett.* **2014**, *113*, 226101.

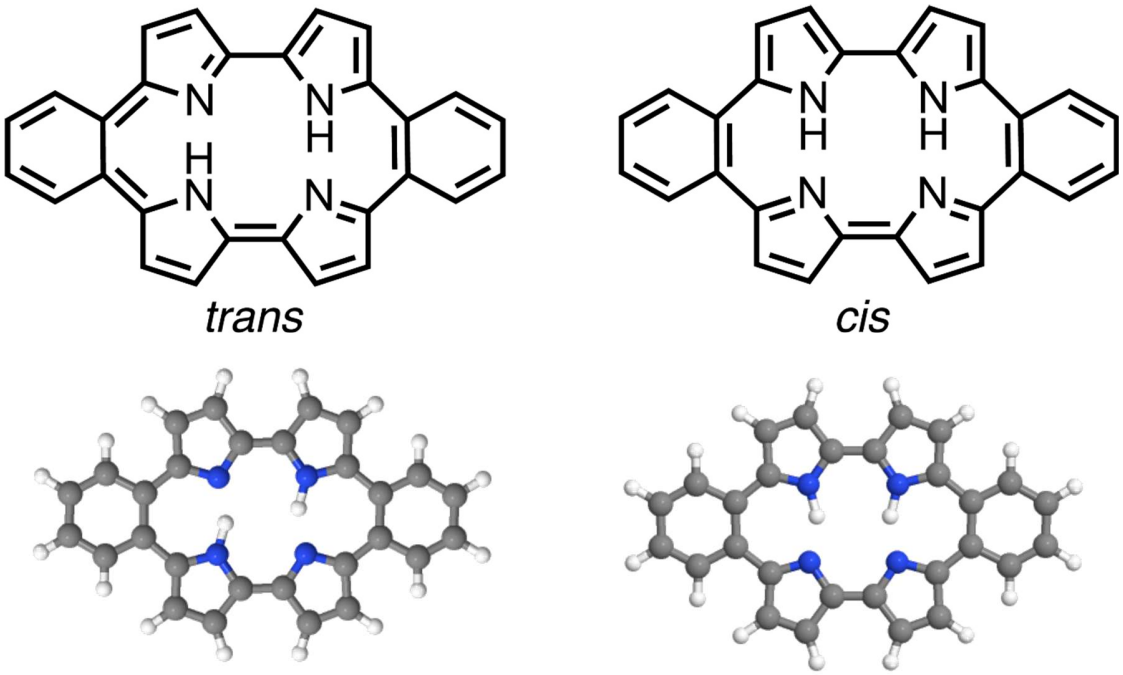

Figure S1. Trans and cis tautomeric forms of *meso*-dibenzoporphycene (mDBPc). Upper panel shows chemical structures and lower panel shows corresponding ball-stick models. The color code for the ball-and-stick model is blue for nitrogen atoms, gray for carbon atoms, and white for hydrogen atoms.

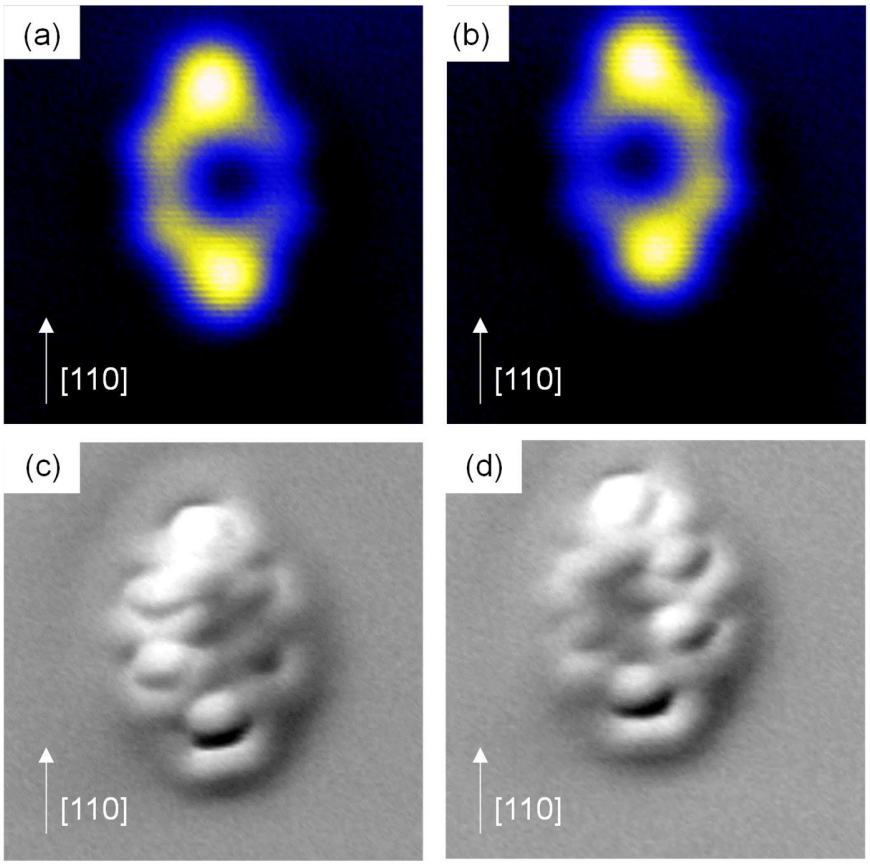

Figure S2. mDBPc molecule adsorbed on the Ag(111) surface. (a and b) Constant-height tunneling current images and (c and d) Δf images of the same molecule before (a and c) and after (b and d) inducing the flip along the molecular long axis by a voltage pulse. Images in (a) and (b) are the same as the ones in Figure 1. The Δf images were acquired by approaching the probe 200 pm towards the surface from the distance at which the tunneling current images were measured. Image size is (2.5 nm × 2.5 nm). Sample bias was V_s=100 mV for (a) and (b), and V_s=10 mV for (c) and (d), respectively. I_t color scale: 2.2-10.7 pA. (c and d) Δf gray scale: –0.63 to +0.47 Hz.

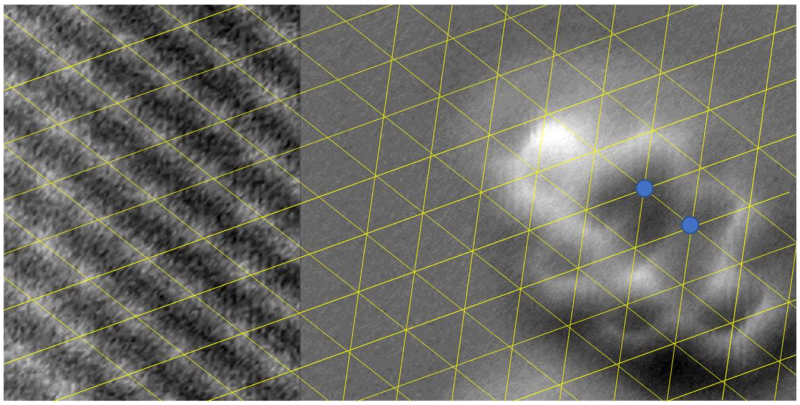

Figure S3. The same image as Fig. 1c with lattice grid superimposed to the Ag atomic positions. The Ag atoms that are involved in the interaction with the mDBPc molecule are marked by blue dots.

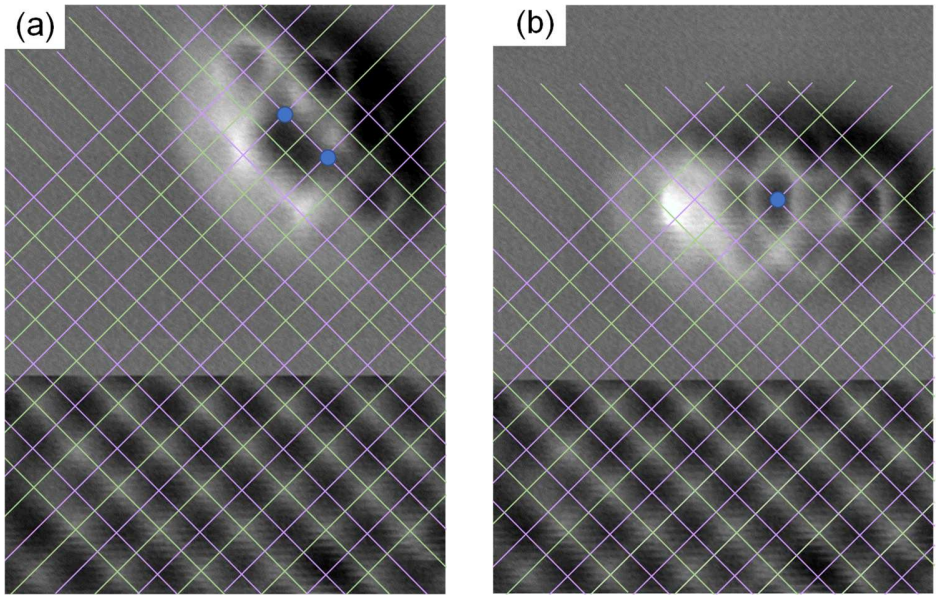

Figure S4. The same images as Fig. 3 with lattice grids superimposed over the NaCl latomic positions. The light green lines lay over the Cl sites, and the purple lines highlights the Na sites (the bright protrusions in the Δf images correspond to Cl atoms). The Na positions that are involved in the interaction with the mDBPc molecule are indicated by blue dots.

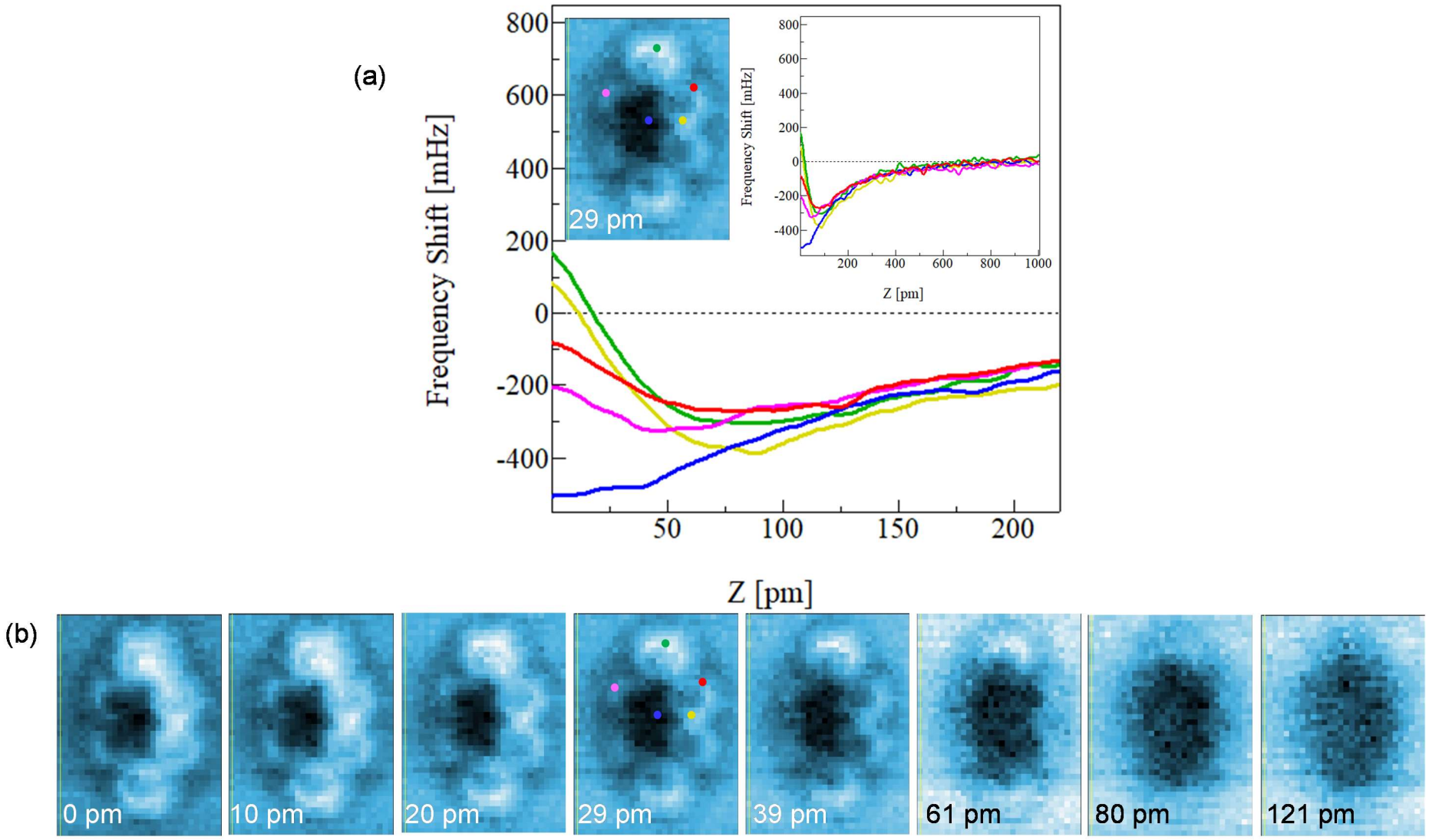

Figure S5. (a) Frequency shift (Δf) vs. distance (z) curves extracted from a force volume measured over a mDBPc molecule on the Ag(111) surface. The origin in the distance axis corresponds to the closest approach of the probe towards the molecule. The inset show the curves over the whole separation range explored. The color code for the curves and the corresponding acquisition location in the image is the same. The force volume comprised (30 × 40) curves of 512 points each covering a (1.5 nm × 2 nm) surface area. (b) Slices of the force volume at various separations.

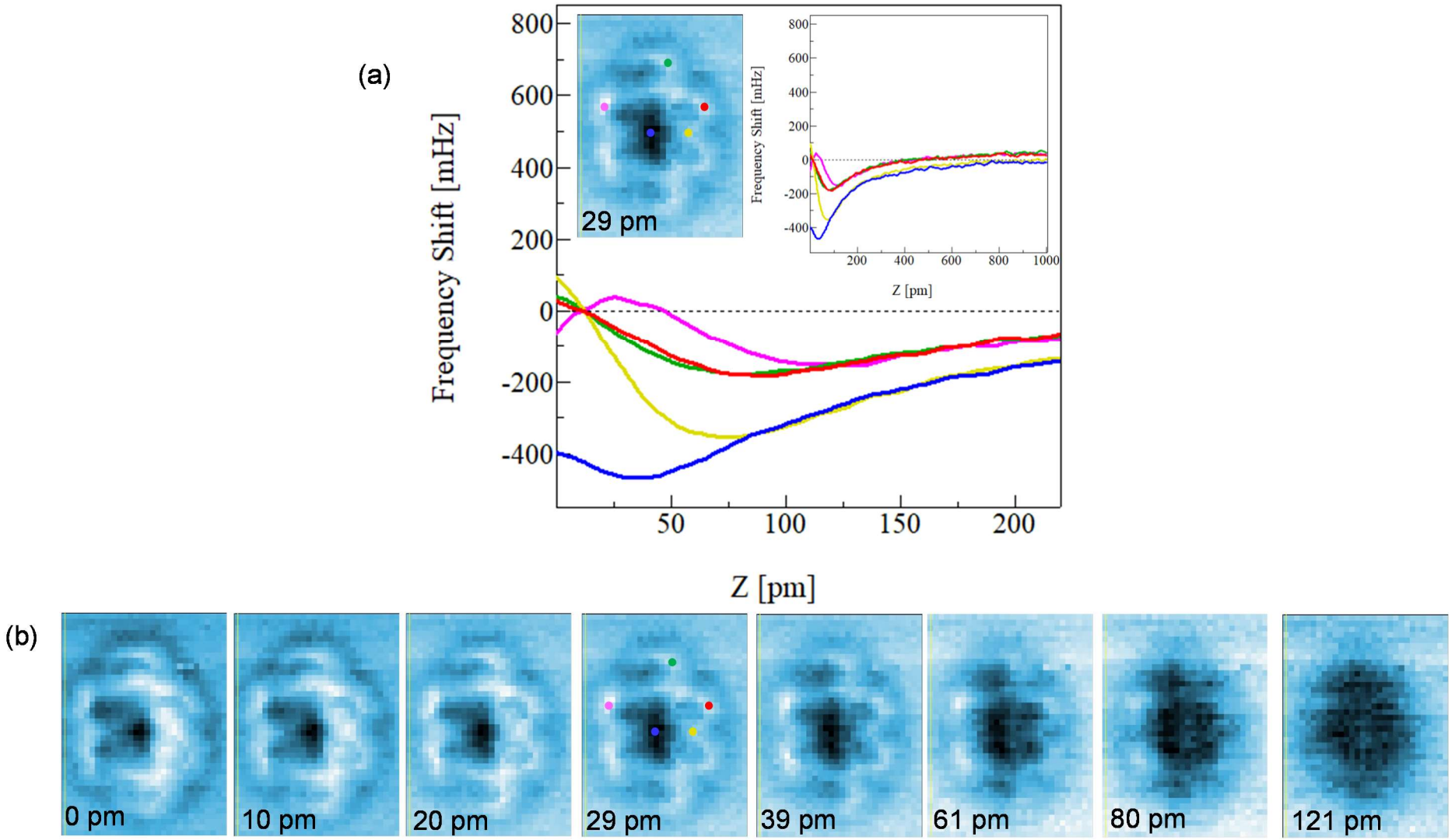

Figure S6. (a) Frequency shift (Δf) vs. distance (z) curves extracted from a force volume measured over a mDBPc molecule in configuration A adsorbed on a bilayer thick NaCl film. The origin in the distance axis corresponds to the closest approach of the probe towards the molecule. The inset show the curves over the whole separation range explored. The color code for the curves and the corresponding acquisition location in the image is the same. The force volume comprised (30 × 40) curves of 512 points each covering a (1.5 nm × 2 nm) surface area. (b) Slices of the force volume at various separations.

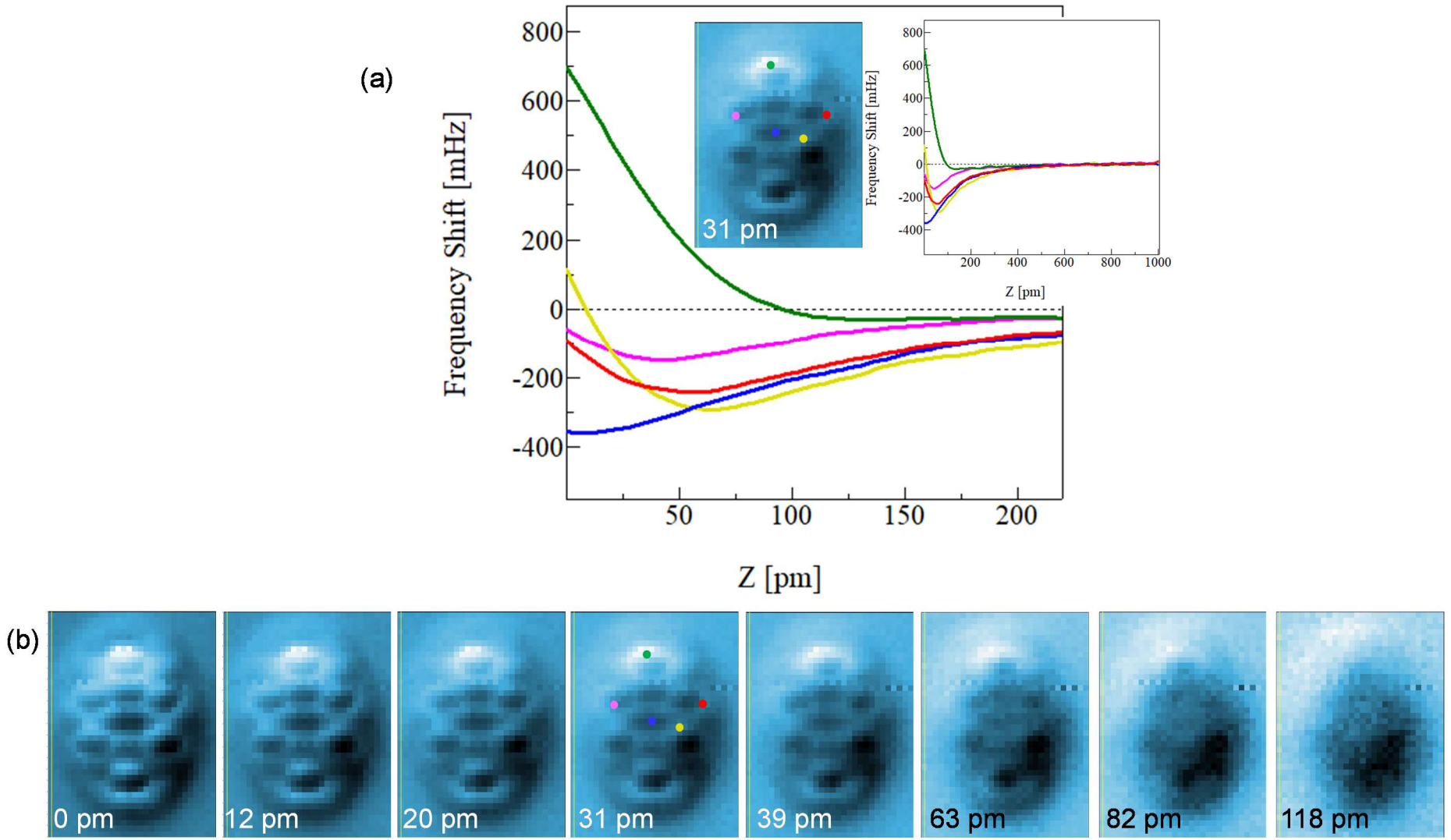

Figure S7. (a) Frequency shift (Δf) vs. distance (z) curves extracted from a force volume measured over a mDBPc molecule in configuration B adsorbed on a bilayer thick NaCl film. The origin in the distance axis corresponds to the closest approach of the probe towards the molecule. The inset show the curves over the whole separation range explored. The color code for the curves and the corresponding acquisition location in the image is the same. The force volume comprised (30 × 40) curves of 256 points each covering a (1.5 nm × 2 nm) surface area. (b) Slices of the force volume at various separations.

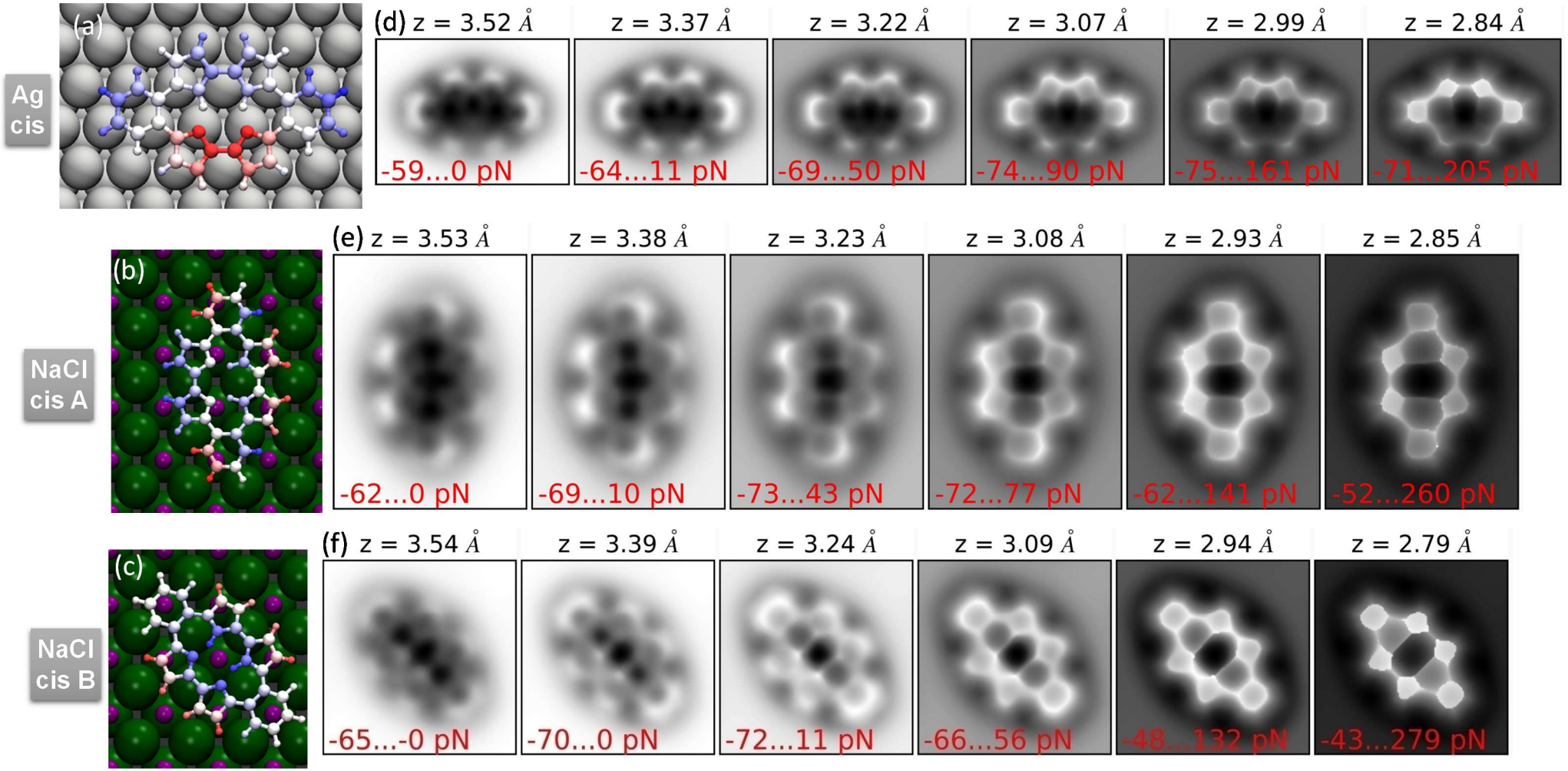

Figure S8. Calculated constant-height force maps of mDBPc molecule on Ag(111) and on NaCl bilayer with six different tip heights. (a, d) *cis*-form of mDBPc on Ag(111), (b, e) *cis*-form of mDBPc in configuration A on NaCl, and (c, f) *cis*-form of mDBPc in configuration B on NaCl.

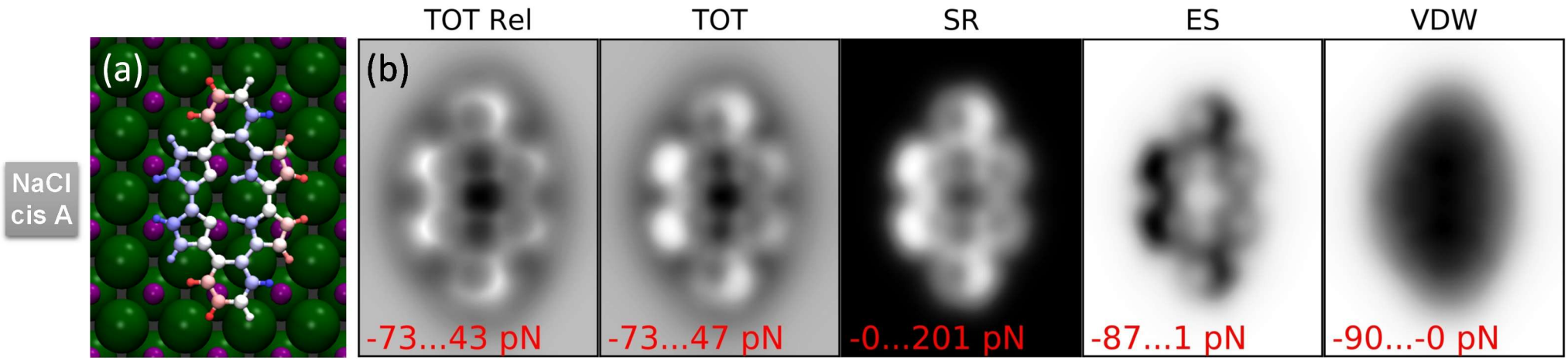

Figure S9. Calculated constant-height force maps of mDBPc molecule on a NaCl bilayer in configuration A with the tip height at 3.1 Å from the average molecular plane. (a) show schematic of adsorption configuration and images in (b) from left to right display spatial maps of total force with relaxation of the probe apex (TOT Rel), total force without relaxation (TOT), short-range force (SR), electrostatic force (ES), and van der Waals force (VDW), respectively.